Reprinted from Applied Optics, Vol. 25, page 209, January 15, 1986

Pulsed-mode laser Sagnac interferometry with applications in nonlinear optics and optical switching

Yao Li, George Eichmann, and R. R. Alfano

A Sagnac interferometer (SI) has been constructed with a mode-locked Nd^{3+}:YAG laser as its source. The advantages in pulsed laser interferometry of using a SI over a Mach-Zehnder interferometer are analyzed. The autostability property of SI is experimentally demonstrated. Applications of an SI to light-induced index of refraction change measurements and to the picosecond optical switching are discussed. Experimental results are presented.

I. Introduction

Over the past two decades, the method of pulse laser interferometry (PLI) has been developed as a diagnostics aid to probe ultrafast phenomena. Early work on PLI dates back to the era of pulsed holography which made it possible to use the interferometric method to measure quantities associated with fast moving objects.[1,2] Since then there has been considerable interest in using the interferometric method to probe short-time phenomena. Work has been performed to diagnose plasma produced by an ultrashort laser pulse.[3,4] One of the advantages of using PLI is that it solves the so-called synchronization problem.[4] Other works using PLI are also available.[5,6] In all these experiments, there is a common problem. Because of the instability of optical components, there is no fixed phase relationship between two interfering beams, i.e., for the same physical condition, fringe patterns due to different laser shots are not identical. As a consequence, most applications are restricted to measurements of single-shot events. Recently, this problem has been overcome using a new technique of combining a Mach-Zehnder-type interferometer (MZI) with an active electronic stabilizing device. The active MZI was used to measure the orientational relaxation time of CS_2.[7] This measurement was accomplished by real-time scanning of the signals resulting from the interference between a reference pulse and the pulse that has undergone an induced refractive-index change caused by a strong laser pulse. The output optical signal is stable because, for different laser shots, a fixed phase relation exists between two interfering beams. However, an electronic feedback control system is needed.

In this paper, a new technique which performs stable ultrashort PLI without the use of an electronic feedback control device is described. The technique is based on the use of a Sagnac interferometer (SI). The applications of SI for measurements of the optical pulse duration and of the material orientational relaxation time will be discussed. For a fixed overlap between the pump and the signal beam at a nonlinear material, the SI output intensity can acquire two stable states. Thus an autostabilized SI device is suitable for a picosecond optical switch.

II. Sagnac Interferometer

For an interferometer, stability is the most important requirement. There are several reported methods[8,9] for stabilizing a cw laser interferometer. These methods, in general, use electronic devices, such as a feedback, a lockin amplifier, and a signal generator, for stabilization. The electronic devices compensate for the changes in the optical path caused by vibrational displacements in the optical elements. In addition to the expense, the method works well only for either cw or high but not for low-repetition-rate pulse lasers.

In most interferometers, the two optical beams traverse distinct optical paths before recombining. While the use of different optical paths has many advantages, unfortunately, it does not allow for autocompensation of unwanted vibrations. This may not

The authors are with City College of New York, New York, New York 10031.

Received 29 July 1985.
0003-6935/86/020209-06$2.00/0.

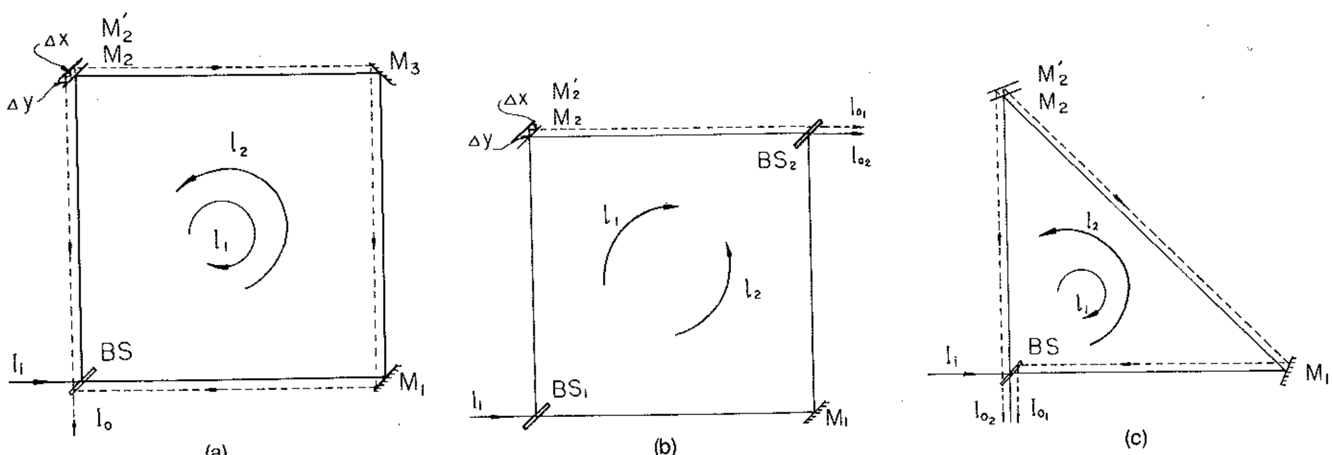

Fig. 1. Vibrational stabilization comparisons between different arrangements of interferometers: (a) a rectangular SI; (b) a rectangular MZI; (c) a triangular SI: M, mirror; BS, beam splitter; Δx,Δy, translational shift of a mirror caused by vibration; and I_i,I_O, input and output intensities.

be the case for a SI.[10] Here the two interfering beams travel along identical optical path but in opposite directions. The applications of the SI are found in constructing the antiresonant ring lasers, in coupling the laser output as well as in performing the optical inversion.[11-13] The purpose of this section is to show the stability advantage of a SI over that of a MZI.

Consider two different interferometers (see Fig. 1). In Fig. 1(a) a rectangular SI, while in Fig. 1(b) a rectangular MZI are depicted. The solid lines designate the two ideal and identical optical paths ($l_1 = l_2$), where $l_{1,2}$ is the path length of arms 1,2, respectively. When the mirror M_2 suffers a translational shift ($\Delta x;\Delta y$), the new optical path difference in the SI can be expressed as

$$\Delta l_s' = |l_1 - l_2 + 2(\Delta y - \Delta x)| = 2|\Delta y - \Delta x|. \quad (1)$$

While for the same translational shift for a MZI, the two beams cannot recombine at the same point on the beam splitter (BS). When a beam of coherent plane wave with the finite beam width is used, the new optical path difference for the MZI is

$$\Delta l_m' = |l_1 - l_2 + \Delta y| = |\Delta y|. \quad (2)$$

For a purely translational shift Δy should be equal to Δx. Then Eqs. (1) and (2) reduce to $\Delta l_s = 0$, and $\Delta l_m = 2\Delta x$. This result shows that a MZI is more sensitive to vibrations than a SI.

The phase difference between the two interfering beams is[8]

$$\Delta\phi = \frac{1}{c}(\Delta l n\omega + \Delta n l\omega + \Delta\omega n l), \quad (3)$$

where l is the optical path length, n is the index of refraction, ω is the angular frequency of the optical source, and c is the velocity of light. The first term in parentheses is due to a vibrational contribution, while the second and third terms are due to the index of refraction change in one of the optical paths and the frequency shift of the optical source, respectively. When a laser output frequency is stable, i.e., ($\Delta\omega = 0$) and when there is no change in the index of refraction, i.e., ($\Delta n = 0$) in the optical paths, both the second and third terms vanish. Thus a translational shift in the mirror M_2 does not effect the phase difference in a rectangular SI but does affect a MZI even with a coherent plane wave illumination. The common spatial shift of the interference pattern obtained in the outputs of both interferometers is small and negligible. When the input beam is not a coherent plane wave [see Fig. 1(b)], the MZI suffers an additional phase shift. A rectangular-type SI is vibration stabilized as long as it is kept free of rotation, and the vibrational frequency is limited to

$$\Omega_{\max} < \frac{c}{l_p}, \quad (4)$$

where $\Omega_{\max}$ represents the maximum horizontal vibrational frequency, and l_p is the optical loop length. It can be shown that the stability of the other type of SI may not be as good as that of a rectangular-type SI shown in Fig. 1(a). For example, a triangular [see Fig. 1(c)] SI[11,12] can perform the autostabilization only with a coherent plane wave illumination. When the input is not the coherent plane wave, a problem similar to that in a MZI will arise.

Compared to other type interferometers, the SI is easy to align. This fact is especially important in PLI. The use of ultrashort optical pulses requires accurate alignment of the optical elements. In a SI, adjustment is needed only for the counterpropagating beams so that they are incident on the same points on the beam splitter and on all mirrors. However, a SI has the drawback that some optical beams are retroreflected.

III. Measurements Involving Light-Induced Refractive-Index Change in Liquid using a Sagnac Interferometer

According to Eq. (3), a change in the refractive index can cause a change in the phase difference between the two interfering beams. This fact has been widely used in interferometry. For most two-beam interferometers, when only one of the two beams propagates through a material that has undergone an index of refraction change, the interference pattern can be used to analyze this change. However, in a SI, the two interfering beams travel along the identical path. Any slow change probed by one beam will be compensated by the same change probed by the other beam. Thus a SI is not applicable for many usual cw laser interferometric applications, such as the measurement of the index of refraction change. In a pulsed laser operation, however, when one of the two beams undergoes an ultrafast phase change caused by an ultrafast index of refraction change, this change will not be autocompensated. This fact allows probing ultrafast dynamics of a material while benefiting from its vibration stabilization property.

A strong linearly polarized light pulse traveling through an isotropic medium, such as a liquid, causes the medium to be temporally anisotropic resulting in an induced birefringence.[14,15] Unlike an optical Kerr gate, which requires an induced difference between the indices of refraction parallel and perpendicular to the laser polarization vector field,[16,17] the PLI requires only the induced change from the linear refractive index in one direction, either parallel or perpendicular to the polarization of the inducing light field. When one of the two beams in the SI undergoes such an induced refractive-index change, a time-dependent phase shift, proportional to this refractive-index change between the two beams, is obtained.

For a 1-D Gaussian light pulse, the electric field can be expressed as

$$E(z,t) = 2E_0 \exp\left[-\frac{1}{\tau_t^2}\left(t-\frac{z}{v}\right)^2\right]\cos\left[\omega\left(t-\frac{z}{v}\right)\right], \quad (5)$$

where v is the velocity of light in the medium, and τ_t is the pulse temporal width. The time average of this field square can then be expressed as

$$\langle E^2(z,t)\rangle = E_0^2 \exp\left[-\frac{2}{\tau_t^2}\left(t-\frac{z}{v}\right)^2\right]. \quad (6)$$

The induced refractive-index changes, from the linear index of refraction in the parallel and in the perpendicular directions relative to the inducing electric field, are given as[15]

$$\Delta n_\parallel = \frac{3}{2} n_2^e E^2(z,t) + \frac{n_2^0\sqrt{\pi}\tau_t}{3\sqrt{2}\tau_0}\langle E^2(z,t)\rangle \times \operatorname{erfc}\left[\frac{\sqrt{2}}{\tau_t}\left(\frac{z}{v}-t\right)+\frac{\tau_t}{\sqrt{8}\tau_0}\right] \times \exp\left[\frac{2}{\tau_t^2}\left(t-\frac{z}{v}\right)^2+\frac{z-vt}{v\tau_0}+\frac{\tau_t^2}{8\tau_0^2}\right], \quad (7)$$

$$\Delta n_\perp = \tfrac{1}{2} n_2^e E^2(z,t) - \frac{n_2^0\sqrt{\pi}\tau_t}{6\sqrt{2}\tau_0}\langle E^2(z,t)\rangle \times \operatorname{erfc}\left[\frac{\sqrt{2}}{\tau_t}\left(\frac{z}{v}-t\right)+\frac{\tau_t}{\sqrt{8}\tau_0}\right] \times \exp\left[\frac{2}{\tau_t^2}\left(t-\frac{z}{v}\right)^2+\frac{z-vt}{v\tau_0}+\frac{\tau_t^2}{8\tau_0^2}\right], \quad (8)$$

where τ_0 is the mean orientational relaxation time, n_2^e and n_2^0 are the electronic and molecular orientational Kerr coefficients, and erfc [ ] is the complementary error function, respectively. Substituting Eqs. (5) and (6) into Eqs. (7) and (8) and using the assumptions described in Ref. 15, we have, for the parallel and the perpendicular index of refraction changes,

$$\frac{\Delta n_\parallel}{n_2E_0^2} = \begin{cases} \left(\dfrac{3n_2^e}{2n_2}+\dfrac{2\,{}_cn_2^0}{3n_2}\right)\exp(-t'^2) & \tau_0' \ll 1, \\ \dfrac{3n_2^e}{2n_2}\exp(-t'^2)+\dfrac{2\,{}_cn_2^0}{3n_2\tau_0'}\displaystyle\int_{-\infty}^{t'}\exp\left[-\left(s^2+\frac{t'-s}{\tau_0'}\right)\right]ds & \tau_0' \approx 1, \\ \dfrac{3n_2^e}{2n_2}\exp(-t'^2)+\dfrac{{}_cn_2^0\sqrt{\pi}}{3n_2\tau_0'}\exp\left(\dfrac{-t'}{\tau_0'}+\dfrac{1}{4\tau_0'^2}\right) \times \operatorname{erfc}\left(-t'+\dfrac{1}{2\tau_0'}\right) & \tau_0' \gg 1, \end{cases} \quad (9)$$

$$\frac{\Delta n_\perp}{n_2E_0^2} = \begin{cases} \left(\dfrac{n_2^e}{2n_2}-\dfrac{{}_cn_2^0}{3n_2}\right)\exp(-t'^2) & \tau' \ll 1, \\ \dfrac{n_2^e}{2n_2}\exp(-t'^2)-\dfrac{{}_cn_2^0}{3n_2\tau_0'}\displaystyle\int_{-\infty}^{t'}\exp\left[-\left(s^2+\frac{t'-s}{\tau_0'}\right)\right]ds & \tau' \approx 1, \\ \dfrac{n_2^e}{2n_2}\exp(-t'^2)-\dfrac{{}_cn_2^0\sqrt{\pi}}{6n_2\tau_0'}\exp\left(\dfrac{-t'}{\tau_0'}+\dfrac{1}{4\tau_0'}\right) \times \operatorname{erfc}\left(-t'+\dfrac{1}{2\tau_0'}\right) & \tau' \gg 1, \end{cases} \quad (10)$$

where ${}_cn_2^0$ is called the first-order corrected coefficient of n_2^0 and is defined as ${}_cn_2^0 = n_2^0(1+J_a)$ with J_a as the pair correlation factor; $n_2 = n_2^e + n_2^0$ and $\tau_0' = \sqrt{2}\tau_0/\tau_t, t' = \sqrt{2}t/\tau_t$. The induced birefringence is the difference between Eqs. (9) and (10).[15] The three expressions in Eqs. (9) and (10) are approximations where the material orientational relaxation time is much faster, slower, or much slower than the inducing pulse width, respectively. All the first terms in the six expressions in Eqs. (9) and (10) represent purely electronic effect contributions, while all the second terms are molecular orientational effect contributions. A comparison between Eqs. (9) and (10) shows that for the same inducing field the magnitude of $\Delta n_\parallel$ is always greater than that of $\Delta n_\perp$. To maximize the light-induced index of refraction change, one should orient the polarization of the optical beam under induced phase shift, parallel to the polarization of the inducing beam. Figure 2 shows the theoretical curves for liquid CS_2, where the parameters are $n_2^e/n_2 = 0.193$ and $n_2^0/n_2 = 0.807$.

According to the first expression in Eq. (9), when the material orientational relaxation time τ_0 is much less

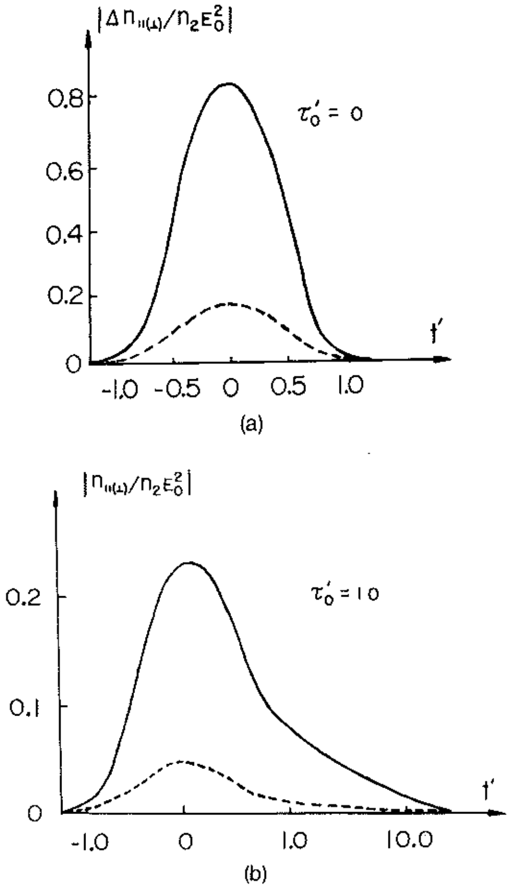

Fig. 2. Calculated curves for light-induced index of refraction changes (absolute value) in CS_2. Solid (dashed) lines are for the changes in the parallel (perpendicular) directions to the laser polarization field. τ_0' is the ratio of the material orientational relaxation time τ_0 over the laser pulse width τ_t, and τ_0' is 0 for (a) and 10 for (b).

than the inducing pulse width τ_t, the change of the refractive index with respected to time is a Gaussian curve characterized by the pulse width τ_t. Thus, when a weak signal pulse is sent through a medium simultaneously with a strong arriving pumping pulse, the signal pulse will probe the maximum of the refractive index. As the time overlap between the two pulses changes, depending on overlap, the signal beam will probe different refractive indices. When a liquid nonlinear material cell is placed in one arm of a SI so that there is a lag time between two arriving counterpropagating pulses, as one of the counterpropagating pulse overlaps with a strong pump pulse, an induced phase difference is produced. To ascertain that the other pulse does not probe this induced index of refraction change, the time difference between the two counterpropagating pulses should be longer than the correlation width between the optical pulse duration τ_t and the material orientational relaxation time τ_0. In this case, the SI will only compensate for the low-frequency vibrations but not for the induced phase difference between the two beams. The interference between the signal and the reference pulse (a pulse which does not undergo any induced refractive-index change) is proportional to a sinusoidal phase difference $\Delta\phi$ function. In the linear region of the sinusoidal curve, i.e., for a small $\Delta\phi$ about an operating point, the interference intensity change will be proportional to $\Delta n_{\parallel}$. In this case, the width of the interference output curve represents the duration of the optical pulse. Thus the optical pulse width can be measured using a PLI.

This method can also be used to measure the orientational relaxation time τ_0 of the material. When the optical pulse width τ_t is less than the material orientational relaxation time τ_0, as is the case in the second expression in Eq. (9), the resultant $\Delta n_{\parallel}$ curve becomes asymmetric [see Fig. 2(b)]. The interference output from a SI, which is proportional to $\Delta n_{\parallel}$, then spreads as a function of the lag time from its peak intensity. In this case, depending on the value of τ_0', the output intensity curve width is broader than the pulse duration. The material orientational relaxation time τ_0 can be deduced from the slope of the curve tail.[7] In general, for such a relaxation time measurement, the ratio τ_0' should be around 10–30. When τ_0' is too large, the orientational contribution of $\Delta n_{\parallel}$ will be completely damped out so that the curve again becomes Gaussian characterized by the optical pulse width.[15]

IV. Sagnac Interferometer as an Optical Switch

Among the many types of optical switch, the optical interference switch has received special interest. Since the phase difference change between the interfering beams can cause in the output intensity either a constructive or destructive interference state, an interferometer is a promising device for switching between the low- and high-energy states. Much attention has been paid to the construction of optical bistable switches[18] using a multiple-beam (Fabry-Perot etalon) interferometer that contains a nonlinear material. These types of device have the following advantages: (1) when the front and back mirrors are fixed together, the etalon has good stability; (2) the alignment is relatively easy and the size of the device, if integrated, can be small; (3) because of the multiple-beam interference phenomenon, the contrast of the two output states can be high. The main reason that other interferometers have not received much attention is due to their alignment and stability difficulties. However, because an autostabilized SI is easy to align, it is well suited for pulsed optical switching.

For a SI optical switch (SIS), there is a fixed temporal overlap between the pump and signal pulses. To guarantee that the SIS switches its energy between the two well-defined (low and high) states, the induced phase difference should be less than or equal to π with the initial (without pumping) output to be in either a constructive or destructive interference state. In an ideal case, the initial output state of the SIS is in a destructive interference state. This is so because the beam traveling in one direction, as compared with the beam traveling in the opposite direction, undergoes an additional air–glass–air reflection.

This additional reflection leads to destructive interference. By slightly misaligning one of the mirrors, however, a constructive interference as the initial state can also be obtained. The switch on (off) time depends on the optical pulse shape and the material orientational relaxation time. In general, when the relaxation time τ_0 is much less than the pulse width τ_t, the switch on and off times are about the same. However, when τ_0 is much larger than τ_t, the switch off time will be much longer than the switch on time. If τ_0 and τ_t are about the same, the switch off time is somewhat longer than the switch on time.

The contrast between low and high output states is an important factor for an optical switch. For good contrast, the two interfering beams should have equal amplitude. For this reason, a 50/50 beam splitter is used. By reducing the physical dimensions, using integrated optics, the constant loop length delay can be reduced. In this case, according to Eq. (4), the stability also improves. In principle, the SIS is cascadable. Therefore, other switching functions such as AND; OR; EXCLUSIVE-OR operations can also be implemented.

V. Experiment

Figure 3 shows our experimental setup. A Quantel mode-locked Nd^{3+}:YAG laser generates two pulses, one at 532- and another at 1064-nm wavelength. The 532-nm pulse is separated by a 50/50 beam splitter (BS) into two parts: with one pulse traveling in a clockwise while the the other pulse travels in a counterclockwise direction. The two pulses recombine at the same point on the BS. Both beams pass through a 1-cm CS_2 cell. A 1064-nm pump pulse is separated by a mirror M_1 that only reflects 1064-nm beam. The beam passes through a delay prism D driven by a Aerotech stepping motor and is then focused to a 1-mm spot in the CS_2 cell. The cell overlap angle between the 1064-nm beam and the 532-nm beam is ~1°. All optical beams are vertically polarized. At distances d_1 and d_2, two HA-30 filters are used to remove the 1064-nm radiation. At the output of the SI, a Hamamatsu S-20 photodiode with a front adjustable aperture is used to collect the interference signal. This signal is displayed on a Tektronix-7104 oscilloscope.

When the 1064-nm pump beam is off, the interference pattern, observed at the output due to the 532-nm beams, contains a few fringes. When at the cell the 1064-nm beam temporally overlaps with one 532-nm beam, such as the counterclockwise beam shown in Fig. 3, a portion of the output fringe shifts. This result is due to the refractive-index change of CS_2 induced by the 1064-nm beam is probed by only one of the 532-nm (counterclockwise) beams. In fact, either one of the 532-nm beams can be chosen to undergo this induced index of refraction change. We used the beam with a longer path length. To have a required time difference between the two 532-nm beams, the cell is positioned asymmetrically. The front aperture of the photodiode is adjusted so that only the changing portion of the output pattern is detected. A delay prism scans the cell overlap between the 1064-nm pump beam and the 532-nm signal beam. The scanned interference signal, is displayed in Fig. 4. The width of the curve is ~33 ps. This width represents the pulse duration of our Nd^{3+}:YAG laser. In general, with CS_2, optical pulse wider than 20 ps can be measured using this method. Our fringe visibility (contrast), defined as $V = (I_{max} - I_{min})/(I_{max} + I_{min})$, is ~52%. Since the SI measurement was performed on a table without vibration isolation, the result shown in Fig. 4 demonstrates the stability of this device.

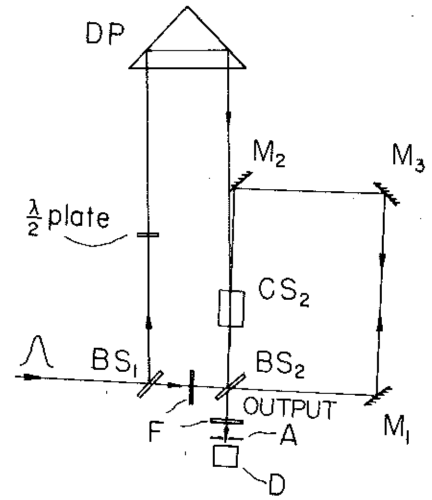

Fig. 3. Experimental setup. The input pulse contains two wavelengths at 1064 (532) nm and M, mirror; BS, beam splitter; DP, delay prism; F, filter. λ/2 plate, halfwave plate, A, adjustable aperture; and D, detector.

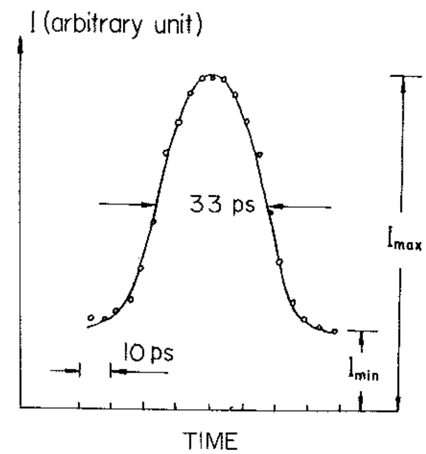

Fig. 4. Output intensity curve obtained by scanning the overlap between pulses at CS_2 cell vs delay time.

VI. Summary and Conclusion

In this paper, it has been verified because of its autostability and its ease of alignment that a Sagnac interferometer is a promising device for pulse interferometry and optical switching. The major advantage of this device is that the scan, which is often required in real-time measurements, can easily be performed without the use of an electronic stabilization system. The experimental result demonstrated that the system stability was good even on a conventional unisolated table. Real-time applications in light-induced index of refraction change in liquid measurements have been discussed. The experimental measurement of the pulse width of a mode-locked Nd^{3+}:YAG laser was presented. Also the possibility of using SIS to build optical switching elements was proposed. The construction of optical switching networks is indicated.

This work was supported in part by a grant from the Air Force Office of Scientific Research.

References

1. J. W. Goodman, "Temporal Filtering Properties of Holograms," Appl. Opt. **6**, 857 (1967).
2. J. D. Redman, "Holographic Velocity Measurement," J. Sci. Instrum. **44**, 1032 (1967).
3. D. T. Atwood and L. W. Coleman, "Microscopic Interferometry of Laser-Produced Plasma," Appl. Phys. Lett. **24**, 408 (1974).
4. H. Schmidt, H. Salzmann, and H. Strohwald, "Interferometry Using Subnanosecond Pulses from TEA Nitrogen Laser," Appl. Opt. **14**, 2250 (1975).
5. H. Bjelkhagen, "Pulsed Sandwich Hologram Interferometry," J. Opt. Soc. Am. **67**, 1433 (1977).
6. R. Kristal, "Pulsed HF Laser Holographic Interferometry," Appl. Opt. **14**, 628 (1975).
7. J-M. Halbout and C. L. Tang, "Femtosecond Interferometry for Nonlinear Optics," Appl. Phys. Lett. **40**, 765 (1982).
8. P. Shajenko and E. L. Green, "Signal Stabilization of Optical Interferometer Hydrophones by Tuning the Light Source," Appl. Opt. **19**, 1895 (1980).
9. A. Olsson, C. L. Tang, and E. L. Green, "Active Stabilization of a Michelson Interferometer by an Electrooptically Tuned Laser," Appl. Opt. **19**, 1897 (1980).
10. E. J. Post, "Sagnac Effect," Rev. Mod. Phys. **19**, 475 (1967).
11. A. E. Siegman, "An Antiresonant Ring Interferometer for Coupled Laser Cavities, Laser Output Coupling, Mode Locking, and Cavity Dumping," IEEE J. Quantum Electron. **QE-9**, 247 (1973).
12. R. Trutna and A. E. Siegman, "Laser Cavity Dumping Using an Antiresonant Ring," IEEE J. Quantum Electron. **QE-13**, 955 (1977).
13. K. Otsuka, "Nonlinear Antiresonant Ring Interferometer," Opt. Lett. **8**, 471 (1983).
14. P. D. Maker, R. W. Terhune, and C. M. Savage, "Intensity-dependent Changes in Refractive Index of Liquid," Phys. Rev. Lett. **12**, 507 (1964).
15. K. Sala and M. C. Richardson, "Optical Kerr Effect Induced by Ultrashort Laser Pulses," Phys. Rev. A **12**, 1036 (1975).
16. M. A. Duguay and J. W. Hansen, "An Ultrafast Light Gate," Appl. Phys. Lett. **15**, 192 (1969).
17. P. P. Ho and R. R. Alfano, "Optical Kerr Effect in Liquid," Phys. Rev. A **20**, 2170 (1979).
18. P. W. Smith and W. J. Tomlinson, "Bistable Optical Devices, Promise Subpicosecond Switching," IEEE Spectrum **8**, 26 (June 1981).